



HAL
open science

Accounting for frictional contact in an anisotropic damage model based on compliance tensorial variables, illustration on ceramic matrix composites

Emmanuel Baranger

► **To cite this version:**

Emmanuel Baranger. Accounting for frictional contact in an anisotropic damage model based on compliance tensorial variables, illustration on ceramic matrix composites. *International Journal of Damage Mechanics*, 2019, 28 (8), pp.1150-1169. 10.1177/1056789518812932 . hal-03914216

HAL Id: hal-03914216

<https://hal.science/hal-03914216>

Submitted on 28 Dec 2022

HAL is a multi-disciplinary open access archive for the deposit and dissemination of scientific research documents, whether they are published or not. The documents may come from teaching and research institutions in France or abroad, or from public or private research centers.

L'archive ouverte pluridisciplinaire **HAL**, est destinée au dépôt et à la diffusion de documents scientifiques de niveau recherche, publiés ou non, émanant des établissements d'enseignement et de recherche français ou étrangers, des laboratoires publics ou privés.

Accounting for frictional contact in an anisotropic damage model based on compliance tensorial variables, illustration on ceramic matrix composites

Journal Title

XX(X):2-22

©The Author(s) 2018

Reprints and permission:

sagepub.co.uk/journalsPermissions.nav

DOI: 10.1177/ToBeAssigned

www.sagepub.com/



Emmanuel Baranger ¹

Abstract

Ceramic matrix composites have good thermo-mechanical properties at high or very high temperatures. The modeling of the crack networks associated to the degradation of such composites using damage mechanics is not straight forward. The main reason is the presence of a crack network mainly oriented by the loading direction, which is a priori unknown. To model this, compliance tensorial damage variables are used in a thermodynamic potential able to account for crack closure effects (unilateral contact). The damage kinematic is initially completely free and imposed by the evolution laws. The key point of the present paper is to account for friction in such cracks that can result in an apparent activation/deactivation of the shear damage. The initial model is enriched with an inelastic strain and a friction law. The plasticity criterion is expressed only using tensorial variables. The model is identified and illustrated on multi-axial data obtained at ONERA on tubes loaded in tension and torsion.

Keywords

CMC, anisotropic damage, crack closure, friction, tensorial variables

List of symbols

\mathbb{C}_0	Initial compliance tensor
$\Delta\mathbb{C} = \Delta\mathbb{C}_m, \Delta\mathbb{Z} = \Delta\mathbb{Z}_m$	Damage compliance tensors
$\mathbb{C} = \mathbb{C}_0 + \Delta\mathbb{C}$	Current compliance tensor
$\mathbb{H} = \mathbb{C}^{\frac{1}{2}}, \Delta\mathbb{H} = \Delta\mathbb{C}^{\frac{1}{2}}$ and $\mathbb{H}_0 = \mathbb{C}_0^{\frac{1}{2}}$	see appendix
$\rho\Psi^{el}$	State potential, ρ is the volumic mass
$\langle \cdot \rangle_+, \langle \cdot \rangle_-$	Classical positive and negative parts (see appendix)
$\boldsymbol{\sigma}, \boldsymbol{\sigma}_+, \boldsymbol{\sigma}_-$	Stress, positive part of the stress w.r.t. \mathbb{H} negative part of the stress w.r.t. \mathbb{H}_0 (see appendix)
$\boldsymbol{\varepsilon}, \boldsymbol{\varepsilon}^{el}, \boldsymbol{\varepsilon}^{st}$	Total, elastic and stored strains
$\mathbb{Y}', \mathbb{Y}', \mathbb{Y}''$	Thermodynamical forces or equivalent
\otimes	Tensor product
:	Contracted product between 2nd order tensors
::	Contracted product between 4th order tensors
$(\cdot)_{sym}$	Symmetric part of a second order tensor
\mathbb{I}	Fourth order identity tensor
\dot{a}	Total time derivative of a quantity a

Introduction

Ceramic matrix composites (CMC) are good candidates for the manufacturing of aeronautical engine structures or nuclear energy applications as they present very good specific properties at high temperatures and irradiations. In both cases, engineers have to use mechanical models in order to design and size parts with limited safety factors. Regarding SiC/SiC composites, several crack networks can develop depending on the densification of the material and of the fiber/matrix interface [Guillaumat and Lamon \(1993\)](#). Among them, inter-yarn cracks may develop orthogonally to the loading direction as mentioned by [Aubard \(1992\)](#).

Such damage kinematics have led to the development of the so-called anisotropic damage models in the literature [Kachanov \(1992\)](#); [Ju \(1990\)](#). The introduction of damage variables to describe the effects of crack networks is generally done using the effective stress concept. It has been initiated by [Kachanov \(1958\)](#); [Rabotnov \(1969\)](#) for scalar variables. The problem is more difficult while using tensorial damage variables as in

¹LMT, ENS-Cachan, CNRS, Université Paris-Saclay, France

Corresponding author:

Emmanuel Baranger, LMT, ENS-Cachan, CNRS, Université Paris-Saclay, 61 avenue du président Wilson, F-94235 Cachan, France.

Email: baranger@lmt.ens-cachan.fr

Murakami and Ohno (1981). For example, in Murakami (1988); Betten (1983), a second order damage tensor is used. In order to construct the effective stress, a fourth order effect tensor is built on the basis of this damage description. A difficulty resides in keeping the symmetries of the obtained stress tensor. While an equivalence in strain is generally used, Cordebois and Sidoroff (1979) proposed a solution to that problem assuming an equivalence in energy. This solution has been followed by Voyiadjis and Park (1997) and Park and Voyiadjis (1998) for finite strains. Note that Chaboche (1977) worked on the direct use of a fourth order damage tensor to define an effective stress. Ladevèze (2002) does not use this concept of effective stress and directly postulates the form of the damaged potential.

Another major problem is to account for crack closure effects i.e. restauration of the stiffness in compression. Important for CMCs like in Gasser et al. (1996), this problem of stiffness recovery in compression is also well known in the field of brittle or quasi-brittle material modeling (Halm and Dragon (1998); Lemaitre et al. (2000) for e.g.). The difficulty resides in the obtention of continuous stress/strain relations i.e. convex potential for multi-axial non-proportional loadings Chaboche (1992); Carol and Willam (1996). For that, two main approaches have been developed for CMCs. The first one is to discretize the potential crack directions in the plane and use associated scalar damage variables in fixed directions as in Marcin et al. (2011); Bernachy-Barbe et al. (2015a). The second one is to use tensorial damage variables. The simplest approach is to use a second order tensor damage variable as in Chaboche and Maire (2001); Gasser et al. (1996). Several difficulties associated to the model of Chaboche and Maire are mentioned in Cormery and Weleman (2002) and by the authors themselves. Another approach is to use directly fourth order tensors as in Chaboche (1982). For example, Ladevèze (2002) used compliance tensors as damage variables. He defined associated special positive and negative parts of the stresses in order to get a free energy potential convex regarding the stress to respect the conditions given by Curnier et al. (1994). This model from Ladevèze is the basis of this paper. Note that, full tensorial damage models have been simplified to scalar damage models in the litterature, for example Chaboche and Maire (2001) leads to Marcin et al. (2011). An automatic strategy adapted to that purpose can be found in Baranger (2013); Friderikos and Baranger (2016).

As already mentioned, the model initially developed by Ladevèze (2002), relies on the use of 4th order tensorial variables as damage variables. The damage kinematics is therefore completely free and only imposed by the evolution laws. This model has been extended to take into account non-proportional multi-axial loadings recently Baranger (2016). In this last paper, the history effect of damage is extended to account for turning crack orientations that have been observed during alternate torsion tests by Bernachy-Barbé (2014). This rich experimental study is used as validation but does not exhibit the effect of crack closure on the shear stiffness. Indeed, Maire and Pacou (1996) have performed tension/compression/torsion tests on SiC/SiC tubes and exhibited the recovery of the shear stiffness while cracks are loaded in compression. This effect is associated to friction in existing cracks. Following the work of Andrieux et al. (1986), some authors Halm and Dragon (1998); Ragueneau et al. (2000) added a model of plasticity to account

for friction in cracks. [Chaboche and Maire \(2001\)](#) also introduced this mechanism but using an activation/deactivation rule similar to unilateral contact. As mentioned by the authors, this leads to some difficulties regarding loading cycles because an infinite friction coefficient is implicitly assumed. The different proposed models generally use damage variables working in directions explicitly given by some eigenvectors which give the damage directions. In that context, it is difficult to get good properties for turning loading directions. The model proposed by Ladevèze does not use such explicit directions given by eigenvectors. In this paper, we propose to integrate friction in this model.

In this paper, the original model from [Ladevèze \(2002\)](#) is presented in the next section. A first illustration of this model is shown on CMC. In the second section, a simple case is used to better understand how to take into account sliding based on the work of [Andrieux et al. \(1986\)](#). In the third section the model is written in a more complex case and illustrated in the fourth section for data from [Maire and Pacou \(1996\)](#) and on a complex loading case.

Original damage model

In order to introduce versatile damage kinematics, different authors have chosen to describe damage using fourth order tensors [Chaboche \(1982\)](#); [Ju \(1990\)](#). In this part, the model from Ladevèze for SiC/SiC composites is emphasized [Ladevèze \(2002\)](#); [Cluzel et al. \(2009\)](#); [Genet et al. \(2014\)](#). The first main idea of this model is to let the damage kinematic completely free a priori and to specify it using the evolution laws. The second idea is to split the contributions related to the different crack networks. The objective is to have a mechanical model that could be linked to a physico-chemical one to treat self-healing aspects of lifetime predictions [Cluzel et al. \(2009\)](#); [Genet et al. \(2012\)](#); [Baranger \(2017\)](#). The present paper will focus only on the mechanical part of the model. The identification and validation of the model focuses on the data of [Maire and Pacou \(1996\)](#), only the part of the model related to degradation mechanisms present in the experimental data are presented hereafter that simplifies the model.

State potential and damage variables

The elastic potential $\rho\Psi^{el}$ is written in stress as the sum of three contributions: the first is a contribution only active in tension, the second is a contribution active only in compression and the third is a contribution active both in tension and compression (i.e. mainly shear). It reads:

$$\rho\Psi^{el} = \frac{1}{2}\sigma_+ : \mathbb{C} : \sigma_+ + \frac{1}{2}\sigma_- : \mathbb{C}_0 : \sigma_- + \frac{1}{2}\sigma : \Delta\mathbb{Z} : \sigma \quad (1)$$

$\Delta\mathbb{C} = \mathbb{C} - \mathbb{C}_0$ and $\Delta\mathbb{Z}$ are the damage variables of the model, by definition they are positive and have the symmetries of a compliance tensor so that the associated tensors \mathbb{H} and \mathbb{H}_0 exist. σ_+ and σ_- are positive and negative parts of the stress σ defined to manage unilateral contact in cracks (the shear stiffness recovery is not taken into account in this form as it is related to friction) and to keep a convex potential in stress even for non-proportional loadings. For that, two spectral decompositions are used. The first is

used to define the positive part:

$$\boldsymbol{\sigma}_+ = \mathbb{H}^{-1} : \langle \mathbb{H} : \boldsymbol{\sigma} \rangle_+ \quad (2)$$

The second is used to define the negative part:

$$\boldsymbol{\sigma}_- = \mathbb{H}_0^{-1} : \langle \mathbb{H}_0 : \boldsymbol{\sigma} \rangle_- \quad (3)$$

This leads to:

$$\rho\Psi^{el} = \frac{1}{2} \langle \mathbb{H} : \boldsymbol{\sigma} \rangle_+ : \langle \mathbb{H} : \boldsymbol{\sigma} \rangle_+ + \frac{1}{2} \langle \mathbb{H}_0 : \boldsymbol{\sigma} \rangle_- : \langle \mathbb{H}_0 : \boldsymbol{\sigma} \rangle_- + \frac{1}{2} \boldsymbol{\sigma} : \Delta\mathbb{Z} : \boldsymbol{\sigma} \quad (4)$$

With the proposed positive and negative parts, the state potential is convex with respect to $\boldsymbol{\sigma}$ as demonstrated in [Ladevèze et al. \(2014\)](#). It allows to get a continuous stress-strain relation even during crack closure. Note that the use of classical positive and negative parts on the stress ($\langle \boldsymbol{\sigma} \rangle_+$ and $\langle \boldsymbol{\sigma} \rangle_-$) would lead to a non-convex potential and thus to a non-continuous stress-strain relation. Note also that, contrary to the classical positive and negative part, $\boldsymbol{\sigma} \neq \boldsymbol{\sigma}_+ + \boldsymbol{\sigma}_-$.

The stress-strain relation is given by (see appendix of [Baranger \(2013\)](#) for some calculus elements):

$$\boldsymbol{\varepsilon}^{el} = \frac{\partial \rho\Psi^{el}}{\partial \boldsymbol{\sigma}} = \mathbb{C} : \boldsymbol{\sigma}_+ + \mathbb{C}_0 : \boldsymbol{\sigma}_- + \Delta\mathbb{Z} : \boldsymbol{\sigma} \quad (5)$$

The total damage is split in different contributions related to the different crack networks (inter-yarn cracks, intra longitudinal yarn cracks, intra transverse cracks for example) as in [Cluzel et al. \(2009\)](#). In the following, only the inter-yarn crack network is supposed (noted with underscore m). It is sufficient to describe the experimental results in the present paper. A more detailed experimental investigation (as in [Bernachy-Barbe et al. \(2015b\)](#)) would be necessary to clearly connect the damage contributions to crack networks. In the general case, the total damage is the sum of the different contributions. The associated damage contributions are called: $\Delta\mathbb{C}_m$ and $\Delta\mathbb{Z}_m$ (see [Cluzel et al. \(2009\)](#) for other contributions). In the present paper, we assume that:

$$\Delta\mathbb{C} = \Delta\mathbb{C}_m, \quad \Delta\mathbb{Z} = \Delta\mathbb{Z}_m \quad (6)$$

Thermodynamical forces

The thermodynamical forces associated to the damage variables are also fourth order tensors:

$$\mathbb{Y} = \frac{\partial \rho\Psi^{el}}{\partial \Delta\mathbb{Z}} = \frac{1}{2} \boldsymbol{\sigma} \otimes \boldsymbol{\sigma} \quad (7)$$

$$\mathbb{Y}' = \frac{\partial \rho\Psi^{el}}{\partial \Delta\mathbb{C}} = \frac{1}{2} \boldsymbol{\sigma}_+ \otimes \boldsymbol{\sigma}_+ \quad (8)$$

Another force is introduced to deal with shear:

$$\mathbb{Y}'' = \frac{1}{2}(\mathbf{O}_{\frac{\pi}{2}} \cdot \boldsymbol{\sigma}_+)_{sym} \otimes (\mathbf{O}_{\frac{\pi}{2}} \cdot \boldsymbol{\sigma}_+)_{sym} \quad (9)$$

where $\mathbf{O}_{\frac{\pi}{2}}$ is a $\frac{\pi}{2}$ rotation in the plane. For the moment, the model is defined only for 2D applications.

Damage evolution laws

To build the damage evolution laws, an equivalent driving force is introduced as:

$$z_m(\mathbb{Y}') = ((1 - a)Tr[\mathbb{Y}'^{n+1}] + aTr[\mathbb{Y}'^{n+1}])^{\frac{1}{n+1}} \quad (10)$$

A version written in strain also exists and is commented in [Baranger \(2016\)](#). a allows to pass from isotropic to anisotropic damage and n to emphasize the directionality of damage. In the present case $n = 1$ and thus z_m is positive.

The maximum force over time is defined by:

$$\bar{z}_m(t) = \sup_{\tau \leq t} z_m(\mathbb{Y}'(\tau)) \quad (11)$$

This last equation is used in the following for its simplicity. It leads to an isotropic history that is not relevant for alternate torsion for example as shown in [Baranger \(2016\)](#). In this paper, the author also proposed a version that is adapted to such non-proportional loadings. Regarding the data from Maire and Pacou, this extension is not necessary and will not be presented to keep the model as simple as possible for the reader. The evolution laws read:

$$\Delta \dot{\mathbb{C}}_m = \dot{\alpha}_m \frac{(1 - a)\mathbb{Y}'^n + aTr[\mathbb{Y}'^n]\mathbb{I}}{\bar{z}_m^n} \quad (12)$$

$$\Delta \dot{\mathbb{Z}}_m = \dot{\alpha}_m \frac{b\mathbb{Y}'^m}{\bar{z}_m^n} \quad (13)$$

$\alpha_m(\bar{z}_m)$ is a scalar increasing function. For a unidirectional loading, the reader can check that the damage kinematics given by the evolution laws are in agreement with cracks oriented by the loading direction for $a = 0$. This choice is made in the following. The proposed model leads to a positive dissipated power [Genet et al. \(2014\)](#). The dissipated power $\dot{\omega}$ reads:

$$\dot{\omega} = \Delta \dot{\mathbb{C}}_m :: \mathbb{Y}' + \Delta \dot{\mathbb{Z}}_m :: \mathbb{Y} \quad (14)$$

As shown in [Baranger \(2016\)](#), $\Delta \dot{\mathbb{C}}_m$ is proportional to the derivative of $z_m(\mathbb{Y}')$ so this first part of the dissipated power is always positive. To prove that the second part is always positive, one has to remark that \mathbb{Y}'' has $(\mathbf{O}_{\frac{\pi}{2}} \cdot \boldsymbol{\sigma}_+)_{sym}$ as the only eigendirection associated to a non-zero eigenvalue. Furthermore, this eigenvalue is positive (it is a square). Thus, \mathbb{Y}''^n is proportional to \mathbb{Y}'' with a positive proportionality coefficient (noted

λ) . This leads to:

$$\Delta \dot{Z}_m :: \mathbb{Y} = \dot{\alpha}_m \frac{b \mathbb{Y}'''_m}{\bar{z}_m^n} :: \mathbb{Y} \quad (15)$$

$$= \lambda \dot{\alpha}_m \frac{b \mathbb{Y}''}{\bar{z}_m^n} :: \mathbb{Y} = \lambda \dot{\alpha}_m \frac{b}{4 \bar{z}_m^n} ((\mathbf{O}_{\frac{\pi}{2}} \cdot \boldsymbol{\sigma}_+)_{sym} : \boldsymbol{\sigma})^2 \geq 0 \quad (16)$$

In the following study, all the examples are treated with the stress evolution prescribed. Thus, the strain evolution is determined by the governing equations of the model. The standard procedure leading to the computation of the stress (and tangent stiffness) from the strain and strain increment has not been studied for the moment.

Illustration

First note that, many eigenvalue problems have to be solved due to the positive and negative parts ; this is in general time consuming. In the present case, as in [Cluzel et al. \(2009\)](#); [Baranger et al. \(2011\)](#), a very simple explicit scheme is used. The reader can find a more refined integration scheme in [Genet et al. \(2014\)](#). The model being written in stress, it is rather easy to use classical experimental mechanical tests while the model is more difficult to use in a finite element framework. In this part, the initial model is identified on a part of a test performed by Pacou and Maire (test called SiC05). The loading path is described in figure 1. Associated to this loading path, elastic testing loadings are intercalated between damaging cycles to be able to identify the evolutions of the compliance. These test cycles are shown in figure 2. In this part, related to identification, the combined shear/tension loadings are not used. The strain-stress curve associated to the incremental loading in tension is plotted in figure 3. Figure 4 presents the stress-strain curves related to pure tensile and torsion loadings used to determine the evolution of the compliance tensor between damaging tension incremental loads. For the tensile part, it can be seen that at some point around $-20MPa$ crack closure occurs and the material recovers its initial stiffness. The fact that cracks do not close at zero stress is related to a thermal expansion coefficients mismatch that leads to an initial internal stress state after a manufacturing process done at high temperature. It is not the case in shear, crack lips are slipping. The proposed model is able to account for crack closure effects as shown in the figure 5. The model is formulated to model crack closure at zero stress. This is the reason why, in this last figure, the axial experimental data have been shifted of about $20MPa$ to avoid to add a shifting term in the model as in [Marcin et al. \(2011\)](#). There is no difficulty for that but wouldn't help the reader. In this figure, dashed lines correspond to the identification of the model. The material parameters are given in table 1.

In figure 6, the response for a combine tension/torsion loading is presented. The crack closure effect is visible in the left picture. Note, in the right picture, that the shear stiffness is recovered for negative shear loadings. This loading range also corresponds to a compressive loading range. The shear stiffness recovery is due to friction in the crack lips that are in contact and do not slip. The proposed model, in its initial form, is not able to describe this mechanism. Unilateral contact is modeled but not friction. The

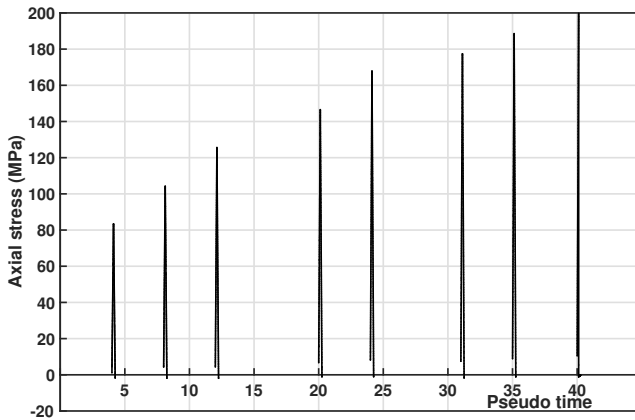


Figure 1. Loading path of an incremental test in tension from Maire and Pacou (1996).

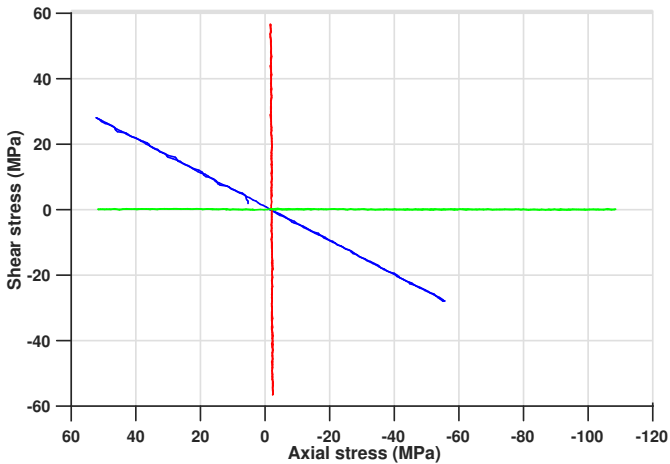


Figure 2. Low amplitude multi-axial loadings for compliance extraction from Maire and Pacou (1996). The green line corresponds to a pure tension/compression loading, the red line corresponds to a pure shear loading and the blue line corresponds to a tension/compression and shear loading.

response of the initial model would be similar to the one in the right side of figure 5. This is the object of the extension proposed in this paper.

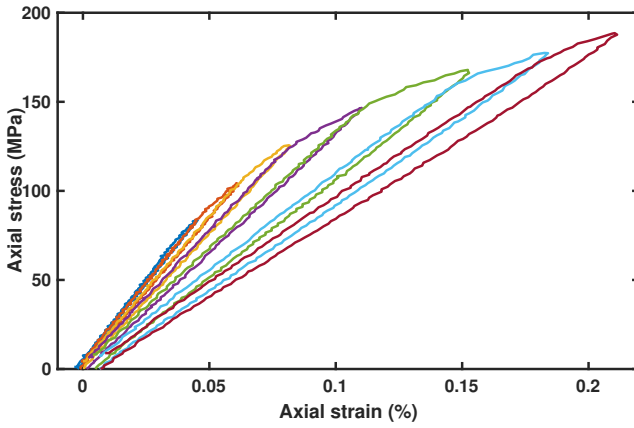


Figure 3. Strain-stress curve of the incremental damaging tension loading part.

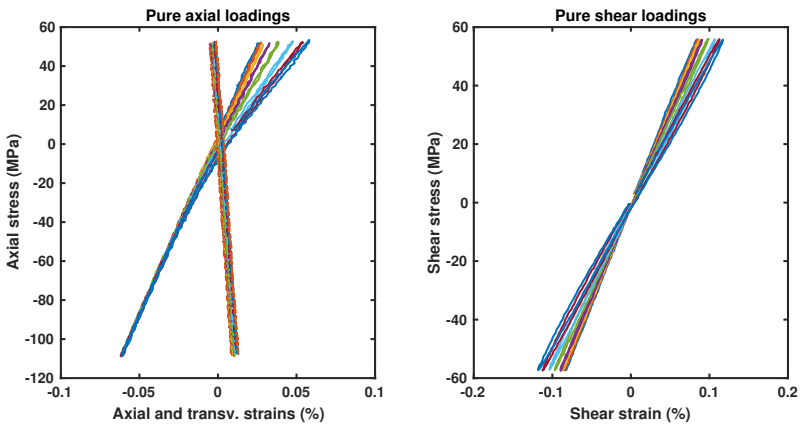


Figure 4. Strain-stress curves of loadings used to determine the compliance evolutions.

Parameter	Value
E (longitudinal Young's modulus)	180 GPa
G (shear modulus)	68 GPa
ν (Poisson's ratio)	0.15
a	0
n	1
b	2
$\alpha_m(z_m)$	$4.10^{-10} (< \sqrt{z_m} - 100MPa >_+)^2 (GPa MPa^2)^{-1}$

Table 1. Material parameters and laws identified.

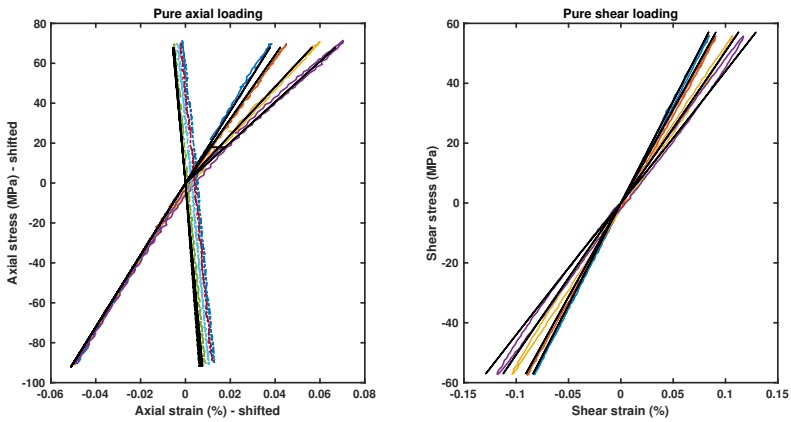


Figure 5. Results of the identification procedure in black (experimental curves in color).

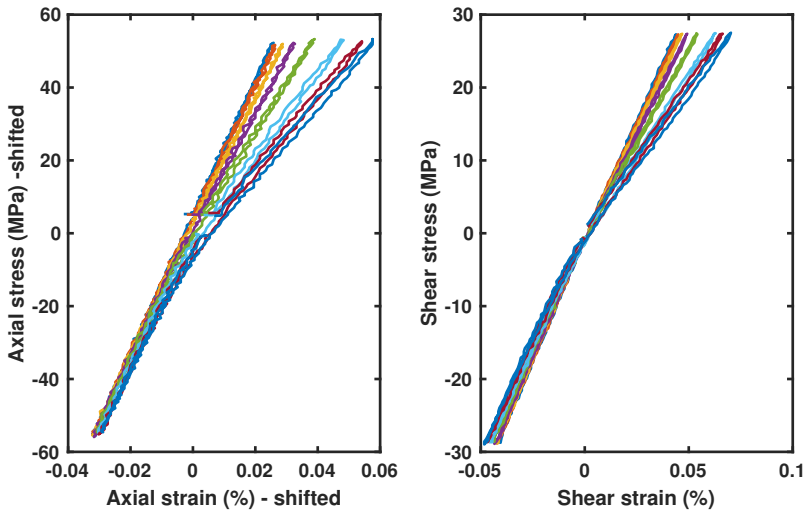


Figure 6. Mechanical response of a tension/torsion combined loading.

Macroscopic Coulomb's criterion in cracks

In [Andrieux et al. \(1986\)](#), a hardening variable is introduced to describe the load transferred by shear between the crack lips while loaded in compression. A similar approach is followed here. A macroscopic hardening variable is introduced as a second order tensor \mathbf{R} . The building and understanding of the evolution laws associated to

friction in existing cracks is illustrated on two simple cases in this section. For the sake of simplicity, in the following $a = 0, n = 1$.

Model development for an initially uni-axial damage state

As a very first case, it is assumed that a preliminary loading has been performed in the direction \underline{n} . Introducing $\mathbf{V}_{nn} = \underline{n} \otimes \underline{n}$, the positive part of the stress during this preliminary phase reads:

$$\boldsymbol{\sigma}_+ = \sigma_{nn} \mathbf{V}_{nn} \quad (17)$$

This is not exactly a uniaxial loading as damage intervenes through \mathbb{H} in the definition of the positive part, nevertheless the initial state of damage is given by:

$$\Delta \mathbb{C}_m = \alpha_1 \mathbf{V}_{nn} \otimes \mathbf{V}_{nn} \quad (18)$$

α_1 is the value taken by α_m at the end of this preliminary loading step. Introducing the orthogonal vector \underline{t} to \underline{n} :

$$\underline{t} = \mathbf{O}_{\frac{\pi}{2}} \cdot \underline{n} \quad (19)$$

where $\mathbf{O}_{\frac{\pi}{2}}$ is the in-plane $\frac{\pi}{2}$ rotation. Introducing $\mathbf{W}_{nt} = (\underline{t} \otimes \underline{n})_{sym}$, we have also:

$$\Delta \mathbb{Z}_m = b\alpha_1 \mathbf{W}_{nt} \otimes \mathbf{W}_{nt} \quad (20)$$

During the next loading step, a non damaging load is assumed. This implies that $\Delta \mathbb{C}_m$ and $\Delta \mathbb{Z}_m$ do not evolve and so continue to model correctly the preliminary crack network. The loading direction does not need to be \underline{n} . The normal and tangential stresses to the preliminary crack network read:

$$\sigma_{nn} = \boldsymbol{\sigma} : \mathbf{V}_{nn} \quad (21)$$

$$\sigma_{nt} = \boldsymbol{\sigma} : \mathbf{W}_{nt} \quad (22)$$

Leading to:

$$\sigma_{nm}^2 = \frac{\boldsymbol{\sigma} : \Delta \mathbb{C}_m : \boldsymbol{\sigma}}{\alpha_1} \quad (23)$$

$$\sigma_{nt}^2 = \frac{\boldsymbol{\sigma} : \Delta \mathbb{Z}_m : \boldsymbol{\sigma}}{b\alpha_1} \quad (24)$$

As mentioned, a hardening variable is introduced as a second order tensor \mathbf{R} to model the load transferred by shear, the projection of this variable on \mathbf{W}_{nt} is noted:

$$r_{nt} = \mathbf{R} : \mathbf{W}_{nt} \quad (25)$$

Note the following equality:

$$(\sigma_{nt} - r_{nt})^2 = \frac{(\boldsymbol{\sigma} - \mathbf{R}) : \Delta \mathbb{Z}_m : (\boldsymbol{\sigma} - \mathbf{R})}{b\alpha_1} \quad (26)$$

$\sigma_{nt} - r_{nt}$ is used to model the frictional stress in the cracks. Assuming a crack in compression, the normal and tangential stresses must satisfy the Coulomb's friction model as:

$$(\sigma_{nt} - r_{nt})^2 - c\sigma_{nn}^2 \leq 0 \text{ if } \sigma_{nn} \leq 0 \quad (27)$$

c is the square of the friction coefficient. Once again, $\sigma_{nt} - r_{nt}$ models the shear stress on the crack lips (the normal stress on the cracks lips is equal to σ_{nn} as shown in [Bui \(1978\)](#)). In terms of macroscopic quantities, the criterion reads:

$$(\boldsymbol{\sigma} - \mathbf{R}) : \Delta\mathbb{Z}_m : (\boldsymbol{\sigma} - \mathbf{R}) - bc\boldsymbol{\sigma} : \Delta\mathbb{C}_m : \boldsymbol{\sigma} \leq 0 \text{ if } \sigma_{nn} \leq 0 \quad (28)$$

In tension, the crack is opened and therefore:

$$\sigma_{nt} - r_{nt} = 0 \implies (\boldsymbol{\sigma} - \mathbf{R}) : \Delta\mathbb{Z}_m : (\boldsymbol{\sigma} - \mathbf{R}) = 0 \quad (29)$$

These last two equations can be combined in a single one. In order to get a convex criterion, a new negative part is introduced via $\Delta\mathbb{H}_m = \Delta\mathbb{C}_m^{\frac{1}{2}}$. Now the criterion reads:

$$(\boldsymbol{\sigma} - \mathbf{R}) : \Delta\mathbb{Z}_m : (\boldsymbol{\sigma} - \mathbf{R}) - bc < \Delta\mathbb{H}_m : \boldsymbol{\sigma} >_- : < \Delta\mathbb{H}_m : \boldsymbol{\sigma} >_- \leq 0 \quad (30)$$

This form will be used in the following for more complex initial states.

Model understanding for an initially bi-axial orthotropic damage

To better understand the results of the previously formulated inequality for an initially multi-axial state, two orthogonal vectors \underline{n}_1 and \underline{n}_2 such as $\underline{n}_1 \cdot \underline{n}_2 = 0$ are considered. These vectors are supposed to be the eigenvectors of the preliminary loading positive stress.

$$\mathbf{V}_1 = \underline{n}_1 \otimes \underline{n}_1, \mathbf{V}_2 = \underline{n}_2 \otimes \underline{n}_2 \quad (31)$$

$$\mathbf{W}_1 = (\underline{t}_1 \otimes \underline{n}_1)_{sym}, \mathbf{W}_2 = (\underline{t}_2 \otimes \underline{n}_2)_{sym} \quad (32)$$

Because the problem is posed in 2D, one can remark that:

$$\mathbf{W}_1 = -\mathbf{W}_2 = \mathbf{W} \quad (33)$$

The initial damage state reads:

$$\Delta\mathbb{C}_m = \alpha_1 \mathbf{V}_1 \otimes \mathbf{V}_1 + \alpha_2 \mathbf{V}_2 \otimes \mathbf{V}_2 \quad (34)$$

$$\Delta\mathbb{Z}_m = b\alpha_1 \mathbf{W}_1 \otimes \mathbf{W}_1 + b\alpha_2 \mathbf{W}_2 \otimes \mathbf{W}_2 \quad (35)$$

leading to:

$$\boldsymbol{\sigma} : \Delta\mathbb{Z}_m : \boldsymbol{\sigma} = b\alpha_1 (\boldsymbol{\sigma} : \mathbf{W}_1)^2 + b\alpha_2 (\boldsymbol{\sigma} : \mathbf{W}_2)^2 = b(\alpha_1 + \alpha_2) (\boldsymbol{\sigma} : \mathbf{W}) \quad (36)$$

The normal stress $\sigma_{n_1 n_1}$ (resp. $\sigma_{n_2 n_2}$) on the crack lips for the crack network oriented by the direction \underline{n}_1 (resp. \underline{n}_2) appears as a contribution in:

$$\begin{aligned} \langle \Delta \mathbb{H}_m : \boldsymbol{\sigma} \rangle_- : \langle \Delta \mathbb{H}_m : \boldsymbol{\sigma} \rangle_- = & \alpha_1 \underbrace{\langle \boldsymbol{\sigma} : \mathbf{V}_1 \rangle_- : \langle \boldsymbol{\sigma} : \mathbf{V}_1 \rangle_-}_{\langle \sigma_{n_1 n_1} \rangle_-^2} \\ & + \alpha_2 \underbrace{\langle \boldsymbol{\sigma} : \mathbf{V}_2 \rangle_- : \langle \boldsymbol{\sigma} : \mathbf{V}_2 \rangle_-}_{\langle \sigma_{n_2 n_2} \rangle_-^2} \end{aligned} \quad (37)$$

because:

$$\Delta \mathbb{H}_m = \sqrt{\alpha_1} \mathbf{V}_1 \otimes \mathbf{V}_1 + \sqrt{\alpha_2} \mathbf{V}_2 \otimes \mathbf{V}_2 \quad (38)$$

The friction criterion (equation 30) and the equations 38, 36 lead to:

$$\begin{aligned} ((\boldsymbol{\sigma} - \mathbf{R}) : \mathbf{W})^2 - c \left(\frac{\alpha_1}{\alpha_1 + \alpha_2} \langle \boldsymbol{\sigma} : \mathbf{V}_1 \rangle_- : \langle \boldsymbol{\sigma} : \mathbf{V}_1 \rangle_- \right. \\ \left. + \frac{\alpha_2}{\alpha_1 + \alpha_2} \langle \boldsymbol{\sigma} : \mathbf{V}_2 \rangle_- : \langle \boldsymbol{\sigma} : \mathbf{V}_2 \rangle_- \right) \leq 0 \end{aligned} \quad (39)$$

From this expression, the reader can note that the normal stress (second part of the left hand side) is here the stress in the directions of the pre-existing cracks weighted by the relative magnitude of damage in each directions.

Anisotropic damage model accounting for unilateral contact and friction

For non orthogonal pre-existing crack networks, the situation is difficult to calculate analytically and no interpretation is given. The proposed form is assumed to remain physically consistent.

The total strain rate is decomposed as:

$$\dot{\boldsymbol{\varepsilon}} = \dot{\boldsymbol{\varepsilon}}^{el} + \dot{\boldsymbol{\varepsilon}}^{st} \quad (40)$$

where $\boldsymbol{\varepsilon}^{st}$ is used to model the frictional sliding in shear.

Expression of the potential and state laws

In the present case, there is only one contribution to \mathbb{Z} and $\mathbb{Z} = \Delta \mathbb{Z}_m$. As friction may occur in all crack networks, \mathbb{Z} will be used in the following. The free energy reads:

$$\rho \Psi = \frac{1}{2} \boldsymbol{\sigma}_+ : \mathbb{C} : \boldsymbol{\sigma}_+ + \frac{1}{2} \boldsymbol{\sigma}_- : \mathbb{C}_0 : \boldsymbol{\sigma}_- + \frac{1}{2} \mathbf{R} : \mathbb{Z} : \mathbf{R} \quad (41)$$

The state laws read:

$$\boldsymbol{\varepsilon}^{el} = \frac{\partial \rho \Psi}{\partial \boldsymbol{\sigma}} = \mathbb{C} : \boldsymbol{\sigma}_+ + \mathbb{C}_0 : \boldsymbol{\sigma}_- \quad (42)$$

$$\boldsymbol{\alpha} = \frac{\partial \rho \Psi}{\partial \mathbf{R}} = \mathbb{Z} : \mathbf{R} \quad (43)$$

This corresponds to the assumption of a linear kinematic hardening law. The forces associated to damage are now defined as:

$$\mathbb{Y} = \frac{1}{2} \mathbf{R} \otimes \mathbf{R} \quad (44)$$

$$\mathbb{Y}' = \frac{1}{2} \boldsymbol{\sigma}_+ \otimes \boldsymbol{\sigma}_+ \quad (45)$$

$$\mathbb{Y}'' = \frac{1}{2} (\mathbf{O}_{\frac{\pi}{2}} \cdot \boldsymbol{\sigma}_+)_{sym} \otimes (\mathbf{O}_{\frac{\pi}{2}} \cdot \boldsymbol{\sigma}_+)_{sym} \quad (46)$$

Damage evolution laws:

First, note that \mathbb{Y} is not used for the inter-yarn matrix damage, it has a contribution for the intra-yarn damage in [Ladevèze \(2002\)](#). The damage evolution laws are supposed to remain unchanged (equations [12](#) and [13](#)).

Coulomb's criterion and flow rule associated to friction:

The Coulomb's criterion is assumed to be:

$$f = (\boldsymbol{\sigma} - \mathbf{R}) : \mathbb{Z} : (\boldsymbol{\sigma} - \mathbf{R}) - bc < \Delta \mathbb{H} : \boldsymbol{\sigma} >_- : < \Delta \mathbb{H} : \boldsymbol{\sigma} >_- \quad (47)$$

The form of this criterion resumes to a friction cone for a unidimensional loading. If there is no compressive stress, then the hardening is equal to the applied stress for the damaged direction.

Proof:

The Kelvin decomposition of $\Delta \mathbb{Z}_m$ reads:

$$\Delta \mathbb{Z}_m = \sum_i \alpha_i \mathbf{V}_i \otimes \mathbf{V}_i \quad (48)$$

Because there is no compressive stress:

$$(\boldsymbol{\sigma} - \mathbf{R}) : \Delta \mathbb{Z}_m : (\boldsymbol{\sigma} - \mathbf{R}) = 0 \quad (49)$$

$$(\boldsymbol{\sigma} - \mathbf{R}) : \Delta \mathbb{Z}_m : (\boldsymbol{\sigma} - \mathbf{R}) = \sum_i \alpha_i ((\boldsymbol{\sigma} - \mathbf{R}) : \mathbf{V}_i)^2 = 0 \quad (50)$$

For i such as $\alpha_i > 0$ (one always has $\alpha_i \geq 0$) then $(\boldsymbol{\sigma} - \mathbf{R}) : \mathbf{V}_i = 0$. Thus:

$$\begin{aligned} \frac{1}{2} \mathbf{R} : \Delta \mathbb{Z}_m : \mathbf{R} &= \frac{1}{2} \sum_i \alpha_i (\mathbf{R} : \mathbf{V}_i)^2 \\ &= \frac{1}{2} \sum_i \alpha_i (\boldsymbol{\sigma} : \mathbf{V}_i)^2 \\ &= \frac{1}{2} \boldsymbol{\sigma} : \Delta \mathbb{Z}_m : \boldsymbol{\sigma} \end{aligned} \quad (51)$$

End of proof.

The flow rules derives from:

$$g = (\boldsymbol{\sigma} - \mathbf{R}) : \Delta \mathbb{Z}_m : (\boldsymbol{\sigma} - \mathbf{R}) \quad (52)$$

The flow rules read:

$$\dot{\boldsymbol{\epsilon}}^{st} = \dot{\gamma}^{st} \frac{\partial g}{\partial \boldsymbol{\sigma}} = \dot{\gamma}^{st} \Delta \mathbb{Z}_m : (\boldsymbol{\sigma} - \mathbf{R}) \quad (53)$$

$$\dot{\boldsymbol{\alpha}} = -\dot{\gamma}^{st} \frac{\partial g}{\partial \mathbf{R}} = \dot{\gamma}^{st} \Delta \mathbb{Z}_m : (\boldsymbol{\sigma} - \mathbf{R}) = \dot{\boldsymbol{\epsilon}}^{st} \quad (54)$$

Classical Kuhn-Tucker conditions should be added. Note that the notion of effective stress is already included in $\boldsymbol{\sigma} - \mathbf{R}$ in shear. Regarding the normal loading, there is no need for the notion of effective stress, the crack is closed or opened. Considering the dissipation related to this plasticity model, as the flow rule derives from a convex function which is positive and nul at the origin, the dissipation is positive [Lemaitre and Chaboche \(1994\)](#).

In the following study, all the examples are treated with the stress evolution prescribed. Thus, the strain evolution is determined by the governing equations of the model. The standard procedure leading to the computation of the stress (and tangent stiffness) from the strain and strain increment has not been studied for the moment.

Applications

Shear stiffness recovery for proportional shear/compression loadings

In this part, the proposed model is applied to the experimental results of Pacou and Maire. Experimental results do not allow to identify the friction coefficient but only to give a bound. This bound is related to the loading ratio of 0.5 between the applied shear stress and the axial stress. To get friction, it is assumed that $c = 0.5$. This choice is arbitrary. Because the experimental data can be described by a stress driven evolution, it is possible to calculate damage independently of friction leading to a very simple solving scheme because the plasticity model is also driven by the stress once the damage is known. The figure 9 shows the stress/strain curves for the combined shear and tension loading

conditions. The model is superimposed to experimental results. On the left picture, the modeled axial behavior is in agreement with the experimental data. Note that even if this picture is similar to the figure 5, loading conditions are not the same. Figure 5 is for identification and the present one for validation. In the right picture of figure 9, the shear behavior is correctly modeled, especially the frictional effect leading to the recovery of the shear stiffness in the compressive loading range. This compressive loading range is defined to account for the shifting of crack closure effect. This is why the shear stiffness recovery is visible for shear stresses less than 5 MPa. The proposed model is thus in good agreement with the existing experimental data. Note the slight discrepancies between the experimental curves and numerical ones ; the author suspects that friction between crack lips leads to an erroneous identification in pure shear and thus leads to an underestimation of the stiffness loss in pure shear.

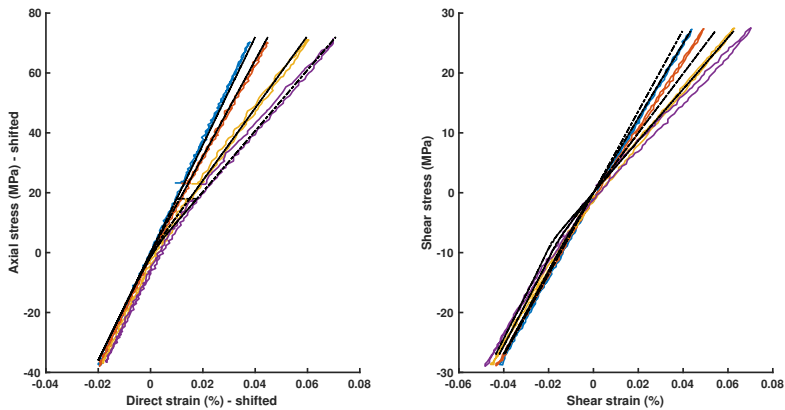


Figure 7. Mechanical response of a tension/torsion combined loading. Continuous colored lines are associated to experimental data while black lines are associated to the model prediction.

Continuous stress/strain evolution for shear/compression non-proportional loadings

In this paragraph, the ability of the model to produce a continuous stress/strain law is evaluated on a complex loading. This one is presented in figure 8. Several phases can be distinguished depending on the pseudo time:

1. from 0 to 2: the tensile stress increases to create damage and is followed by unloading;
2. from 2 to 3: the shear stress increases to create slip between crack lips;
3. from 3 to 4: the shear stress is maintained at its level and a compressive stress is applied so that friction can occur in cracks;

4. from 4 to 5: the compression stress is maintained at its level and the shear stress is decreased to zero;
5. from 5 to 6: the axial stress is increased to go from compression to tension.

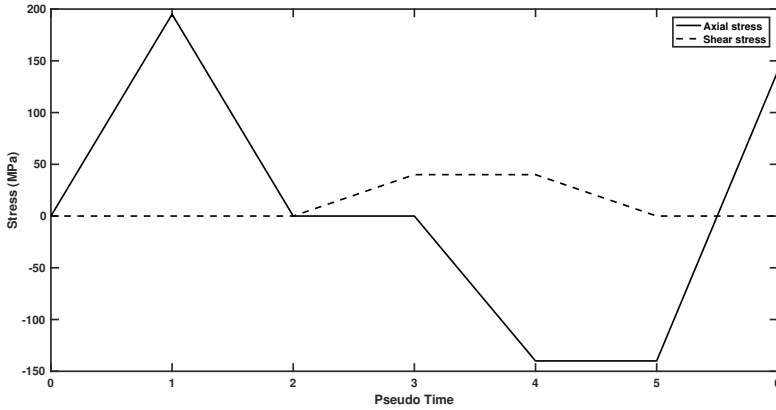


Figure 8. Applied stress in tension/compression and shear.

In figure 9, the total strain resulting from the computation of the model is plotted. The time steps are shown on the shear curve using + symbols. This shows a continuous evolution of the strain versus time. The strain evolution follows the loading phases:

1. from 0 to 1: the slope of variation of the axial strain increases while damage is created;
from 1 to 2: the axial strain decreases elastically;
2. from 2 to 3: the shear strain increases;
3. from 3 to 4: the shear strain remains almost constant, a slight decrease can be observed as the loading direction turns also slightly;
4. from 4 to 5: friction occurs between crack lips, only the elastic part is released. The shear strain decreases to reach a plateau which is the stored part of the strain.
5. from 5 to 6: the axial stress increases to reach zero, the cracks start to slip and the shear strain vanishes when the stress becomes positive.

This test shows the ability of the model to describe continuous stress strain evolutions for complex loadings including friction.

Conclusion

In this work, an anisotropic damage model is proposed to account for all the aspect related to crack closure for SiC/SiC materials i.e. unilateral contact as well as friction. The use of 4th order tensorial damage variables allows to store the information of crack orientations and therefore, a simple plasticity model can be developed to model Coulomb's friction

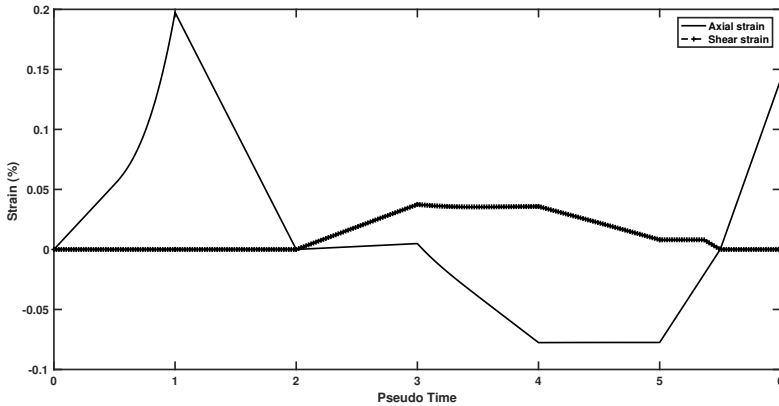


Figure 9. Total strain evolution computed with the model.

in cracks. It relies on the ability to estimate the normal and shear stresses in cracks using a projection of the stress on the damage tensors. Only very few experimental data are available in the literature on CMCs regarding multi-axial loadings and crack closure effects. The data of [Maire and Pacou \(1996\)](#) have been used in this paper to identify the model and check its validity. Non-proportional loading conditions have also been used to show the continuity of the stress-strain law for cracks under complex shear and compression loading sequences. To go further on the study of the interaction between damage development and friction, more experimental data are needed. It would be interesting first to look at available data on reinforced concrete which present similar mechanisms (among many others).

Acknowledgements

The author acknowledges J.-F. Maire and F. Laurin from ONERA for the experimental data. All presented experimental data are extracted from the work of Pacou. This work has only been published in [Maire and Pacou \(1996\)](#).

Spectral decompositions and definitions of positive and negative parts

Kelvin decomposition

Due to the symmetries of a compliance tensor, it is possible using the Voigt's notation to decompose a fourth order tensor as:

$$\mathbb{C} = \sum_i c_i \mathbf{V}_i \otimes \mathbf{V}_i \quad (55)$$

c_i is a positive scalar and \mathbf{V}_i are symmetric tensors of order two. \mathbb{H} is then defined as follows:

$$\mathbb{H} = \mathbb{C}^{\frac{1}{2}} = \sum_i \sqrt{c_i} \mathbf{V}_i \otimes \mathbf{V}_i \quad (56)$$

The same procedure can be done to obtain \mathbb{H}_0 from \mathbb{C}_0 .

Classical positive and negative parts

Starting from the Kelvin decomposition of a second order tensor $\mathbf{a} : \mathbf{a} = \sum_i a_i \underline{v}_i \otimes \underline{v}_i$, the positive and negative parts are defined as:

$$\langle \mathbf{a} \rangle_+ = \sum_i \langle a_i \rangle_+ \underline{v}_i \otimes \underline{v}_i \quad (57)$$

$$\langle \mathbf{a} \rangle_- = \sum_i \langle a_i \rangle_- \underline{v}_i \otimes \underline{v}_i \quad (58)$$

where $\langle \cdot \rangle_+$ (resp. $\langle \cdot \rangle_-$) is the positive (resp. negative) part of a scalar.

Positive and negative parts with respect to damage

$$\boldsymbol{\sigma}_+ = \mathbb{H}^{-1} : \langle \mathbb{H} : \boldsymbol{\sigma} \rangle_+ \quad (59)$$

The second is used to define the negative part:

$$\boldsymbol{\sigma}_- = \mathbb{H}_0^{-1} : \langle \mathbb{H}_0 : \boldsymbol{\sigma} \rangle_- \quad (60)$$

If \mathbb{H}_0 and \mathbb{H} are isotropic then these definitions are equivalent to the classical positive and negative parts.

References

- Andrieux S, Bamberger Y and Marigo JJ (1986) Un modèle de matériau microfissuré pour les bétons et les roches. *Journal de mécanique théorique et appliquée* 5(3): 471–513.
- Aubard X (1992) *Modélisation et identification du comportement mécanique des matériaux composites 2D-C/SiC*. PhD Thesis, Thèse de doctorat: Paris VI.
- Baranger E (2013) Building of a reduced constitutive law for ceramic matrix composites. *International Journal of Damage Mechanics* 22(8): 1222–1238.
- Baranger E (2016) Extension of a fourth-order damage theory to anisotropic history: Application to ceramic matrix composites under a multi-axial non-proportional loading. *International Journal of Damage Mechanics* 27(2): 238 – 252.
- Baranger E (2017) Modeling mechanical behavior of ceramic matrix composites. In: C H Zweben PB (ed.) *Comprehensive Composite Materials II*. Elsevier.

- Baranger E, Cluzel C, Ladevèze P and Mouret A (2011) Effects of the thermomechanical loading path on the lifetime prediction of self-healing ceramic matrix composites. *Science and Engineering of Composite Materials* 18(4): 259–264.
- Bernachy-Barbé F (2014) *Caractérisation des mécanismes d'endommagement et modélisation du comportement mécanique sous chargements multi-axiaux de tubes composites SiC/SiC*. PhD Thesis, Paris, ENMP.
- Bernachy-Barbe F, Gélébart L, Bornert M, Crépin J and Sauder C (2015a) Anisotropic damage behavior of SiC/SiC composite tubes: Multiaxial testing and damage characterization. *Composites Part A: Applied Science and Manufacturing* 76: 281–288.
- Bernachy-Barbe F, Gélébart L, Bornert M, Crépin J and Sauder C (2015b) Characterization of SiC/SiC composites damage mechanisms using digital image correlation at the tow scale. *Composites Part A: Applied Science and Manufacturing* 68: 101–109.
- Betten J (1983) Damage tensors in continuum mechanics. *Journal de Mécanique théorique et appliquée* 2(1): 13–32.
- Bui HD (1978) *Mécanique de la rupture fragile*. Masson.
- Carol I and Willam K (1996) Spurious energy dissipation/generation in stiffness recovery models for elastic degradation and damage. *International Journal of Solids and Structures* 33(20): 2939–2957.
- Chaboche J (1977) Sur l'utilisation des variables d'état interne pour la description du comportement viscoplastique et de la rupture par endommagement. In: *Proc. Problèmes non-linéaires de mécanique, Symposium franco-polonais, Cracow (Poland)*. pp. 137–159.
- Chaboche J (1982) Le concept de contrainte effective appliqué à l'élasticité et à la viscoplasticité en présence d'un endommagement anisotrope. In: *Mechanical Behavior of Anisotropic Solids/Comportement Mécanique des Solides Anisotropes*. Springer, pp. 737–760.
- Chaboche J and Maire J (2001) New progress in micromechanics-based CDM models and their application to CMCs. *Composites Science and Technology* 61(15): 2239–2246.
- Chaboche JL (1992) Damage induced anisotropy: on the difficulties associated with the active/passive unilateral condition. *International Journal of Damage Mechanics* 1(2): 148–171.
- Cluzel C, Baranger E, Ladevèze P and Mouret A (2009) Mechanical behaviour and lifetime modelling of self-healing ceramic-matrix composites subjected to thermomechanical loading in air. *Composites Part A: Applied Science and Manufacturing* 40(8): 976–984.
- Cordebois J and Sidoroff F (1979) Anisotropie élastique induite par endommagement. *Comportement mécanique des solides anisotropes* (295): 761–774.
- Cormery F and Weleman H (2002) A critical review of some damage models with unilateral effect. *Mechanics Research Communications* 29(5): 391–395.
- Curnier A, He QC and Zysset P (1994) Conewise linear elastic materials. *Journal of Elasticity* 37(1): 1–38.
- Friderikos O and Baranger E (2016) Automatic building of a numerical simplified constitutive law for ceramic matrix composites using singular value decomposition. *International Journal of Damage Mechanics* 25(4): 506–537.

- Gasser A, Ladeveze P and Poss M (1996) Damage mechanisms of a woven sic/sic composite: Modelling and identification. *Composites science and technology* 56(7): 779–784.
- Genet M, Marcin L, Baranger E, Cluzel C, Ladevèze P and Mouret A (2012) Computational prediction of the lifetime of self-healing CMC structures. *Composites Part A: Applied Science and Manufacturing* 43: 294–303. DOI:10.1016/j.compositesa.2011.11.004.
- Genet M, Marcin L and Ladeveze P (2014) On structural computations until fracture based on an anisotropic and unilateral damage theory. *International Journal of Damage Mechanics* 23(4): 483–506.
- Guillaumat L and Lamon J (1993) Multi-fissuration de composites sic/sic. *Revue des composites et des matériaux avances* 3: 159–171.
- Halm D and Dragon A (1998) An anisotropic model of damage and frictional sliding for brittle materials. *European Journal of Mechanics-A/Solids* 17(3): 439–460.
- Ju J (1990) Isotropic and anisotropic damage variables in continuum damage mechanics. *Journal of Engineering Mechanics* 116(12): 2764–2770.
- Kachanov L (1958) Time of the rupture process under creep conditions. *Isv. Akad. Nauk. SSR. Otd Tekh. Nauk* 8: 26–31.
- Kachanov M (1992) Effective elastic properties of cracked solids: critical review of some basic concepts. *Applied Mechanics Reviews* 45(8): 304–335.
- Ladevèze P (2002) *An anisotropic damage theory with unilateral effects: applications to laminates and to three-and four-dimensional composites*. O. Allix and F. Hild edition. Elsevier.
- Ladevèze P, Baranger E, Genet M and Cluzel C (2014) *Ceramic Matrix Composites: Materials, Modeling and Technology*, chapter Damage and Lifetime Modeling for Structure Computations. John Wiley & Sons, Inc., pp. 465–519. N. P. Bansal and J. Lamon eds, ISBN: 978-1-118-23116-6, 712 pages.
- Lemaitre J and Chaboche JL (1994) *Mechanics of solid materials*. Cambridge university press.
- Lemaitre J, Desmorat R and Sauzay M (2000) Anisotropic damage law of evolution. *European Journal of Mechanics-A/Solids* 19(2): 187–208.
- Maire J and Pacou D (1996) Essais de traction-compression-torsion sur tubes composites céramique-céramique. In: *JNC 10 : comptes-rendus des dixièmes journées nationales sur les composites*. Paris: AMAC, pp. 1225–1234.
- Marcin L, Maire JF, Carrère N and Martin E (2011) Development of a macroscopic damage model for woven ceramic matrix composites. *International Journal of Damage Mechanics* 20(6): 939–957.
- Murakami S (1988) Mechanical modeling of material damage. *Journal of Applied Mechanics* 55(2): 280–286.
- Murakami S and Ohno N (1981) A continuum theory of creep and creep damage. In: *Creep in structures*. Springer, pp. 422–444.
- Park T and Voyiadjis G (1998) Kinematic description of damage. *Journal of applied mechanics* 65(1): 93–98.
- Rabotnov YN (1969) Creep rupture. In: *Applied mechanics*. Springer, pp. 342–349.
- Ragueneau F, La Borderie C and Mazars J (2000) Damage model for concrete-like materials coupling cracking and friction, contribution towards structural damping: rst uniaxial

application. *Mech. Cohes. Frict. Mater* 5: 607625.

Voyiadjis G and Park T (1997) Anisotropic damage effect tensors for the symmetrization of the effective stress tensor. *Journal of Applied Mechanics* 64(1): 106–110.